Carrier phase delay altimetry with GPS-reflection/occultation interferometry from low Earth orbiters

E. Cardellach,[1] C. O. Ao, M. de la Torre Juárez, and G. A. Hajj

NASA/Jet Propulsion Laboratory, California Institute of Technology, Pasadena, California, USA

Received 20 February 2004; revised 2 April 2004; accepted 16 April 2004; published 26 May 2004.

[1] GPS signals reflected off the surface of the Earth can be detected by receivers aboard occulting Low Earth Orbiters (LEOs). In this work, carrier phase interferometry between the reflected and direct occultation signals is performed to infer its relative delay at centimetric error. Our analysis shows that submeter sensitivity on the surface heights can formally be reached with this technique. The potential applications to polar ice altimetry are discussed. *INDEX TERMS:* 0933 Exploration Geophysics: Remote sensing; 0994 Exploration Geophysics: Instruments and techniques; 1244 Geodesy and Gravity: Standards and absolute measurements; 1863 Hydrology: Snow and ice (1827); 6924 Radio Science: Interferometry. **Citation:** Cardellach, E., C. O. Ao, M. de la Torre Juárez, and G. A. Hajj (2004), Carrier phase delay altimetry with GPS-reflection/occultation interferometry from low Earth orbiters, *Geophys. Res. Lett.*, *31*, L10402, doi:10.1029/2004GL019775.

1. Introduction

[2] During the last decade, several studies have assessed the geophysical content of Global Positioning System (GPS) signals reflected from the surface of the Earth, especially over the ocean. A passive bistatic radar concept, proposed by *Martín-Neira* [1993], would take advantage of the large number of transmitters currently emitting L band coded signals (~30 satellites for the GPS constellation, ~10 for the Russian GLONASS), and the enlargement of the global navigation satellite systems with GALILEO, a European constellation planned for the near-future, to perform multistatic simultaneous observations from ground-air- or space-based platforms, with great spatial and temporal coverage. So far, most experimental work has been focused on applications from ground [*Martín-Neira et al.*, 2001], aircraft [*Garrison et al.*, 1998] or stratospheric balloons [*Cardellach et al.*, 2003], for altimetry and surface roughness measurements [*Zavorotny and Voronovich*, 2000; *Rius et al.*, 2002]. Whereas centimeter precision has been reported for ground-based carrier phase altimetric observations [*Treuhaft et al.*, 2001], and 5-cm for airborne platforms group delay measurements [*Lowe et al.*, 2002b], the altimetric performance from space is still to be clarified. *Lowe et al.* [2002a] described the first GPS reflection gathered from space, while *Beyerle et al.* [2002] identified reflected GPS signal leaking into occultation data collected by a Low Earth Orbiter (LEO). Using radio-holographic technique, *Beyerle et al.* [2002] inferred a precision of ~100 m in the determination of reflection surface heights. This paper is the first to present GPS reflected-to-direct carrier phase interferometry from space-borne receivers. Data from standard GPS LEO occultations with ice-reflection leakage (GPS-R/Occ) are analyzed. The relative delay between the direct and reflected signals are inverted to yield the heights of the reflection points, by taking advantage of the good knowledge of the atmospheric correction, which is the main retrieval product of the GPS LEO occultation instrument. The results suggest that the interferometry technique offers submeter sensitivity to ice topography (see the auxiliary material[1]) with a few km horizontal resolution.

2. Carrier Phase Interferometry

[3] During the last seconds of an occultation, reflected signals may reach the LEO horizon-looking antenna with Doppler frequencies within the receiver bandwidth [*Beyerle et al.*, 2002]. The output of the GPS occultation receiver is the peak of the complex cross-correlation function between the incoming signal and a replica or model of it, and it reproduces the features of the electromagnetic field reaching the antenna. When both the direct and the reflected fields reach the antenna, either the total field or the correlation function, with amplitude A and phase ϕ, can be modeled as

$$Ae^{i\phi} = A_d e^{i\phi_d} + A_r e^{i\phi_r} = e^{i\phi_d}\left[A_d + A_r e^{i(\phi_r - \phi_d)}\right] \quad (1)$$

where A_d and A_r are the amplitudes of the direct and the reflected components, ϕ_d and ϕ_r are their respective phases, with $\phi_d = \phi_0 + k\rho_d$ and $\phi_r = \phi_0 + k\rho_r$, k being the GPS carrier wavenumber, ρ for distance or delay in length units, and ϕ_0 being the initial phase bias. The interferometric phase, $\phi_I = (\phi_r - \phi_d) = k(\rho_r - \rho_d) = k\Delta\rho$ is not a constant during an occultation, thus inducing a fringe pattern in the amplitude and phase of the total field.

[4] The smoothed value of the total field is dominated by the direct contribution, $A_d e^{i\phi_d} \simeq \overline{A} e^{i\overline{\phi}_d} \equiv [\overline{\mathcal{R}}, \overline{\mathcal{I}}]$, where $\mathcal{R}$ stands for its real and $\mathcal{I}$ for its imaginary part. The fringe oscillations around $\overline{A}$ correspond to some projection of the reflected signal. Then, equation (1) becomes

$$Ae^{i\phi} = e^{i\overline{\phi}}\left[\overline{A} + A_r e^{i\phi_I}\right] \equiv [\mathcal{R}, \mathcal{I}] \quad (2)$$

Combining equations (1) and (2) one obtains

$$\tan(\phi_I) = \frac{\overline{\mathcal{R}}\mathcal{I} - \overline{\mathcal{I}}\mathcal{R}}{\overline{\mathcal{R}}(\mathcal{R} - \overline{\mathcal{R}}) + \overline{\mathcal{I}}(\mathcal{I} - \overline{\mathcal{I}})} \quad (3)$$

[1] Currently at Harvard-Smithsonian Center for Astrophysics, Cambridge, Massachusetts, USA.

0094-8276/04/2004GL019775$05.00

[1] Auxiliary material is available at ftp://ftp.agu.org/apend/gl/2004GL019775.

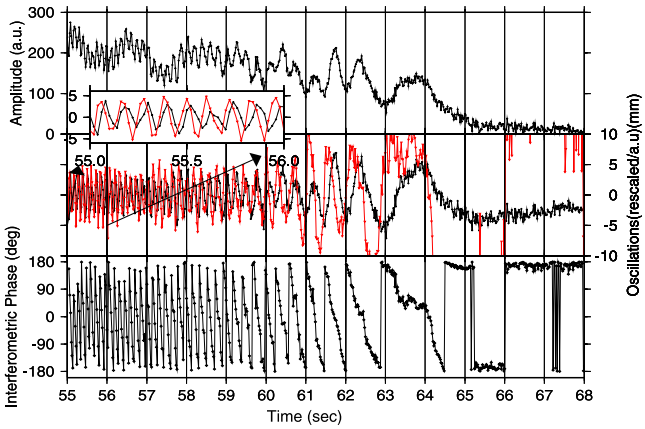

Figure 1. (top) Amplitude of the field as provided by the GPS occultations' receiver. On top of other power modulations (mainly tropospheric effects), the interferometric fringe is detected, with beats oscillating consistently with the frequency analysis: from ~10 Hz at $t = 55$ to very low frequency around the collapse time, $t_c \sim 66$. (middle) Oscillations of both received amplitude and phase around the smoothed values, $A - \overline{A}$ (in black crosses) and $\phi - \overline{\phi}$ (in grey triangles). Units are arbitrary for amplitude (and rescaled respect to the plot above) and mm for phase, a zoom-plot is included for a high frequency interval. The oscillations present the skewed quadrature between amplitude and phase, an indicator of interferometry that contains information about the sense of the interferometric spin. The difficulty of detrending the last portion of cycle of the reflection makes the retrieval unreliable for $t > 64$s. (bottom) Interferometric phase as obtained by application of equation (3) on the data above. All corresponding to CHAMP-GPS51 2001-05-14-01:15 event.

[5] In order to remove non-interferometric modulations, the smoothing is carried out on windows of twice the interferometric period, $T_w = 2T_I = 2/|f_I|$, where $|f_I|$ is estimated from the Fourier analysis of the data: $|f_I| = |f_r - f_d|$. The amplitude as received by the occultation CHAMP-GPS51 2001-05-14-01:15 is displayed in Figure 1 (top). For each cycle added or subtracted in the interferometric phase, the reflected-to-direct delay changes by 1 L1 GPS carrier wavelength, $\lambda \sim 0.19$ m. Because both branches of the signal eventually collapse into a single one, the interferometric carrier phase measurement is not cycle-ambiguous after anchoring to zero at the collapsing time, t_c. The sequence of oscillations in phase residuals are in *skewed quadrature* with respect to the amplitude oscillations (not at 90°, but toward amplitude's minimums, as expected for interferometric behavior), see Figure 1 (middle). This fact supports that these oscillations are interferometric fringes rather than noise or mismodeled modulations. The interferometric phase computed through equation (3) is displayed in Figure 1 (bottom).

[6] Finally, the reflected-to-direct relative delay is obtained from the interferometric phase by aligning the cycles and translating to length units. Data corresponding to $t > 64$s have been rejected, because of the difficulties in appropriately detrending the last interferometric cycle. Instead, the delay is extrapolated toward t_c, and anchored to 0. Uncertainty of 1 second in t_c determination yields to ~1 mm error in the relative delay, which may be considered the formal accuracy of this delay measurement. Figure 2 shows that the procedure results in a few cm formal error, dominated by the sampling resolution of the cycle. The resolution improves along the occultation because the interferometric frequency slows down, enabling better sampling of the cycles. The noise in the receiver tracking loops introduces few mm uncertainty. The carrier phase ambiguity is fixed through the collapsing time, t_c, when $\Delta\rho = 0$, and the cycles are added from that point in reverse order of time.

3. Geophysical Information Content

[7] The reflected-to-direct relative delay may have several contributions. Most of the standard sources of delay in the GPS signal, however, are here canceled because of the differential nature of the observation. Our work assumes that the reflected-to-direct delay, $\Delta\rho$ can be modeled as

$$\begin{aligned}\Delta\rho = \rho^r - \rho^d &= \left(\rho^r_{geo} + \rho^r_{trop} + \rho^r_{rgh} + \rho^r_{iono} + \rho^r_{instr} + n^r\right) \\ &- \left(\rho^d_{geo} + \rho^d_{trop} + \rho^d_{iono} + \rho^d_{instr} + n^d\right) = \Delta\rho_{geo}\left(\vec{R},\vec{T},\vec{S}\right) \\ &+ \Delta\rho_{trop}\left(\vec{R},\vec{T},\vec{S},N\right) + \rho^R_{rgh} + n \end{aligned} \quad (4)$$

The superscripts r and d stand for reflected and direct signals; ρ_{geo} stands for the geometrical delay; ρ_{trop} is the extra delay induced by the troposphere in each ray; ρ_{iono} is the delay introduced by the electronic content of the higher atmosphere; ρ_{instr} are instrumental errors; N is the refractivity profile; and n unmodeled noise. The multipath due to the topography feature of horizontal scales smaller than the Fresnel zone, ~19 km × 1 km, or roughness could also bias the result, ρ_{rgh}. In this preliminary study, we neglect this effect, but keeping in mind that it can be a

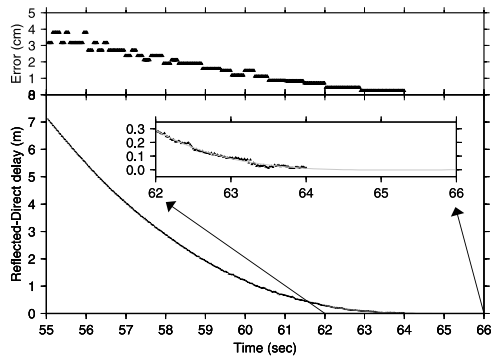

Figure 2. Reflected-to-direct relative delay inferred from the interferometric phase in Figure 1 (bottom). The formal error of this measurement, computed as λ/n (λ for the GPS carrier wavelength and n for the number of samples within 1 interferometric cycle), is displayed on top of the figure. A zoom of the interval used to extrapolate toward the end of the occultation is also included (fit and extrapolation in grey line).

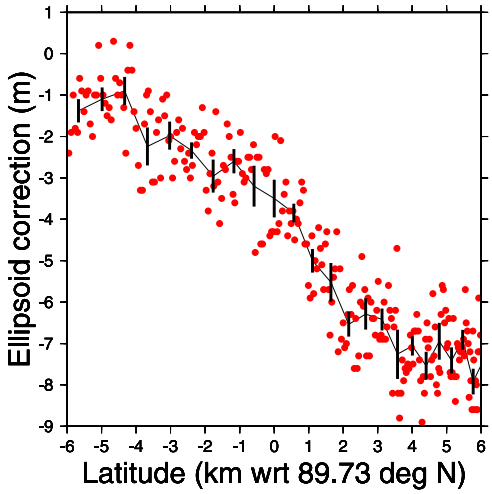

Figure 3. Profile of the elevation of the terrain along the stripe at 20-ms samples (dots) and a 0.2-sec window averages with their RMS dispersion (solid line connecting RMS-bars). The average RMS value is 0.70 m. The horizontal along-track resolution of 0.2-sec average is of the order of 1 km, which is the spacing of the horizontal grid (X-axis centered at 45°E, Y-axis at 89.73°N.)

source of inaccuracies. We also assume the canceling of instrumental and ionosphere perturbations. Under such assumptions, the relative delay is therefore only a function of the locations of the receiver, the transmitter and the specular reflection point $\vec{R}, \vec{T}$ and $\vec{S}$ respectively, along with the refractivity profile of the atmosphere N. The receiver and transmitter locations are known with accuracy better than a few cm, while the refractivity profile is the main retrieval product of the GPS occultation mission. Thus the sole unknown of the system is the location of the specular reflection.

[8] For a given refractivity profile, receiver and transmitter locations and an a priori reference surface, S, the trajectory of both reflected and direct signals may be estimated by a forward ray tracing tool (RTT), providing the location of the specular point and the model for the relative delay: $\Delta\rho_{RTT} = \Delta\rho(S, \vec{R}, \vec{T}, N)$. If the model does not match the data, we can adjust the vertical component of the surface as $S + \delta S$ so that $\Delta\rho_{data} = \Delta\rho_{RTT}(\delta S; S, \vec{R}, \vec{T}, N)$. In this fashion, it is possible to infer the elevation of the reflecting surface with respect to the reference.

3.1. Topographic Profile

[9] In order to generate topographic profiles from the relative delay, the misfit at each 20-ms data sample for different surface height corrections, δS, are computed:

$$M^2(t_i, \delta S) = \frac{\left(\Delta\rho_{data}(t_i) - \Delta\rho_{RTT}(t_i, \delta S; S, \vec{R}, \vec{T}, N)\right)^2}{\sigma^2_{data}(t_i)} \quad (5)$$

where $\sigma_{data}(t_i)$ is the formal error of the delay at the sample t_i. For the inversion of CHAMP-GPS51 2001-05-14-01:15 the range $\delta S = -8.9$ to 0.9 m has been evaluated in steps of 10 cm. The time series altimetric solutions, $\delta S^*(t_i)$, are picked as the surface's elevation that gives a minimum misfit at each t_i. As shown in Figure 3, the 20-ms sampling inversion has uncertainties of the order of ~2 m (range of δS with differences with the data within the data confidence). When smoothing the solution in 0.2-sec windows, the resultant profile has an averaged RMS dispersion of 0.70 m and horizontal spacing of ~1 km, which establishes the formal vertical and horizontal resolutions of the approach.

3.2. Validation

[10] The lack of in-situ data at high polar latitudes hinders the validation of the results. We found a GPS-R/Occ event (CHAMP-GPS39 2003-05-31-19:19) which occurred within two weeks and ~30 km of an Airborne Tropospheric Mapping Lab (ATM) track, cross-comparable with a Digital Elevation Model (DEM) [*Bamber et al.*, 2001]. The ATM precision is of the order of 10 cm, but because of the coarse vertical resolution of the DEM (~10 m RMS accuracy) the GPS interferometric product has been inverted into topographic profiles at 6 m vertical resolution mode. Figure 4 contains the elevation map of the region together with both the airborne laser and GPS-R/Occ altimetric estimates and the interpolation of the DEM under those tracks (top). The gradient of the terrain obtained by GPS-R/Occ agrees with the gradient predicted by DEM with RMS dispersion of 6.6 m, i.e., within the DEM resolution. The GPS-R/Occ to DEM offset is 294 m, same order of magnitude as the ATM to DEM bias for this portion of flight (232 m). The ATM to DEM offset is not a constant value, but changes at different areas/tracks, and the variations are as large as the difference between the ATM and the GPS-R/Occ biases (~60 m). This

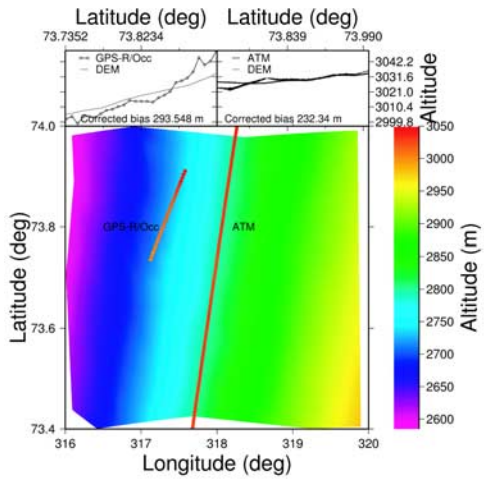

Figure 4. Background: DEM of the region. Tracks: GPS-R/Occ and airborne laser altimeter estimates of the topography, ~30 km and 2-weeks separated measurements. Both have a positive bias with respect to DEM of the same order of magnitude. On top-left: GPS-R/Occ profile and the interpolated DEM profile (with bias removed). The GPS and DEM terrain gradients match with 6.6 m RMS dispersion, which is within the DEM resolution. Top-right: ATM and interpolated DEM profiles (with bias removed).

cross-comparison represents a preliminary proof of concept of GPS-R/Occ as a topographic tool, although dedicated calibration campaigns should be conducted to verify the submeter formal precision that we have achieved with this technique.

4. Discussion and Conclusions

[11] This paper presents the first study on space-based carrier phase interferometric delay between direct and reflected GPS signals. This product, with a few centimeter formal resolution and better formal accuracy, is a differential delay enabling the cancellation of several error terms. This sole achievement opens a new complementary way to process GPS LEO occultation data, with potential geophysical applications in tropospheric refractivity and surface's altimetry. The sensitivity of this observable to variations of the reflecting surface's elevation has been evaluated.

[12] Two topographic ice-profiles have been generated, which are located at the North Pole (89.73°) and Greenland. The former event has been inverted using a high-resolution approach (10 cm steps), resulting in 0.70 m vertical precision at ~1 km horizontal sampling. The second event, on Greenland, has been inverted in a low-resolution mode and cross-compared with ATM and DEM yielding agreement within the data sources resolution. The validation example presents a preliminary proof of concept for utilizing this kind of measurements as a remote sensing tool for ice topography.

[13] Further validation work is required to assess the roles of noise sources and mismodeled parameters. Future work is also intended to determine the spatial-temporal coverage of the ice reflection events and to evaluate the performance of the technique on ocean reflections. Potential application of the interferometric technique for refining the refractivity profiles of the lower troposphere will also be considered. The analysis of archives of past occultation data could be of great interest for the scientific community, filling a temporal and spatial gap on polar regions back to 1995 (GPS-MET, CHAMP, SAC-C). The improvement of receiver tracking to enhance the measurements of the reflection events could also be tackled, especially in views of its impact on upcoming missions, such as COSMIC [*Lee et al.*, 2001] or ACE+ [*Battrick*, 2004] constellations, which will provide an unprecedented rich source of GPR-R/Occ events.

[14] **Acknowledgments.** The research described in this paper was carried out by the Jet Propulsion Laboratory, California Institute of Technology, under contract with the National Aeronautics and Space Administration and a NASA funded National Research Council associateship program. E. C. was an NRC associate at NASA/JPL.

References

Bamber, J. L., R. L. Layberry, and S. P. Gogineni (2001), A new ice thickness and bed data set for the Greenland ice sheet: 1. Measurement, data reduction, and errors, *J. Geophys. Res.*, *106*(D24), 33,773–33,780.

Battrick, B., (Ed.) (2004), ESA Mission Experts Division, Sc. coord. by T. Wehr, in *ACE+ Atmosphere and Climate Explorer*, *Rep. ESA SP-1279(4)*, Eur. Space Agency, Paris.

Beyerle, G., K. Hocke, J. Wickert et al. (2002), GPS radio occultations with CHAMP: A radio holographic analysis of GPS signal propagation in the troposphere and surface reflections, *J. Geophys. Res.*, *107*(D24), 4802, doi:10.1029/2001JD001402.

Cardellach, E., G. Ruffini, D. Pino et al. (2003), MEditerranean Balloon EXperiment: Ocean wind speed sensing from the stratosphere using GPS reflections, *Remote Sens. Environ.*, *88*(3), doi:10.1016/S0034-4257(03)00176-7.

Garrison, J. L., S. J. Katzberg, and M. I. Hill (1998), Effects of sea roughness on bistatically scattered range coded signals from the Global Positioning System, *Geophys. Res. Lett.*, *25*(13), 2257–2260.

Lee, L.-C., C. Rocken, and R. Kursinski (Eds.) (2001), *Applications of Constellation Observing System for Meteorology, Ionosphere and Climate*, Springer-Verlag, New York.

Lowe, S. T., J. L. LaBrecque, C. Zuffada et al. (2002a), First spaceborne observation of an Earth-reflected GPS signal, *Radio Sci.*, *37*(1), 1007, doi:10.1029/2000RS002539.

Lowe, S. T., C. Zuffada, Y. Chao et al. (2002b), 5-cm-precision aircraft ocean altimetry using GPS reflections, *Geophys. Res. Lett.*, *29*(10), 1375, doi:10.1029/2002GL014759.

Martín-Neira, M. (1993), A Passive Reflectometry and Interferometry System (PARIS): Application to ocean altimetry, *ESA Bull.*, *17*, 331–355.

Martín-Neira, M., M. Caparrini, J. Font-Rossello et al. (2001), The PARIS concept: An experimental demonstration of sea surface altimetry using GPS reflected signals, *IEEE Trans. Geosci. Remote Sens.*, *39*(1), 142–150.

Rius, A., J. M. Aparicio, E. Cardellach et al. (2002), Sea surface state measured using GPS reflected signals, *Geophys. Res. Lett.*, *29*(23), 2122, doi:10.1029/2002GL015524.

Treuhaft, R. N., S. T. Lowe, C. Zuffada, and Y. Chao (2001), 2-cm GPS altimetry over Crater Lake, *Geophys. Res. Lett.*, *28*(23), 4343–4346.

Zavorotny, V. U., and A. Voronovich (2000), Scattering of GPS signals from the ocean with wind remote sensing application, *IEEE Trans. Geosci. Remote Sens.*, *38*(2), 951–964.

C. O. Ao, E. Cardellach, M. de la Torre Juárez, and G. A. Hajj, NASA/Jet Propulsion Laboratory, Mail Stop 238-600, 4800 Oak Grove Drive, Pasadena, CA 91109, USA. (chi.o.ao@jpl.nasa.gov; mtj@jpl.nasa.gov; george.a.hajj@jpl.nasa.gov)

E. Cardellach, Harvard-Smithsonian Center for Astrophysics, 60 Garden Street, M.S. 42, Cambridge, MA 02138, USA. (ecardellach@cfa.harvard.edu)